

Simulating starspot activity jitter for spectral types F–M: realistic estimates for a representative sample of known exoplanet hosts

Stefano Bellotti¹, Heidi Korhonen²

¹IRAP, Toulouse (FR), ²European Southern Observatory (CL)



doi <https://doi.org/10.1002/asna.20210003>

stefano.bellotti@irap.omp.eu



Context

Stellar activity represents a serious limitation to exoplanet radial velocity (RV) searches. In fact, surface inhomogeneities due to magnetic activity such as spots produce distortions in the spectral line profiles and therefore spurious RV shifts (known as “jitter”) up to several m/s that drown small planet signals or undermine the accuracy of planetary characterisation. Modelling the spot-driven RV variability is therefore important to design efficient activity-filtering techniques and inform observing strategies.

Our aim is to characterise starspots and simulate the radial velocity curves they induce to determine typical jitter amplitudes for a representative sample of known host stars spanning between F and M spectral type.

Catalog of host stars and simulation sample

We collect information on the $\log R'_{HK}$ activity index from the literature (e.g., [1]) for 218 stars and, due to a lack of data in the temperature range 4000–4500 K, we measure it for ten stars using archival data.

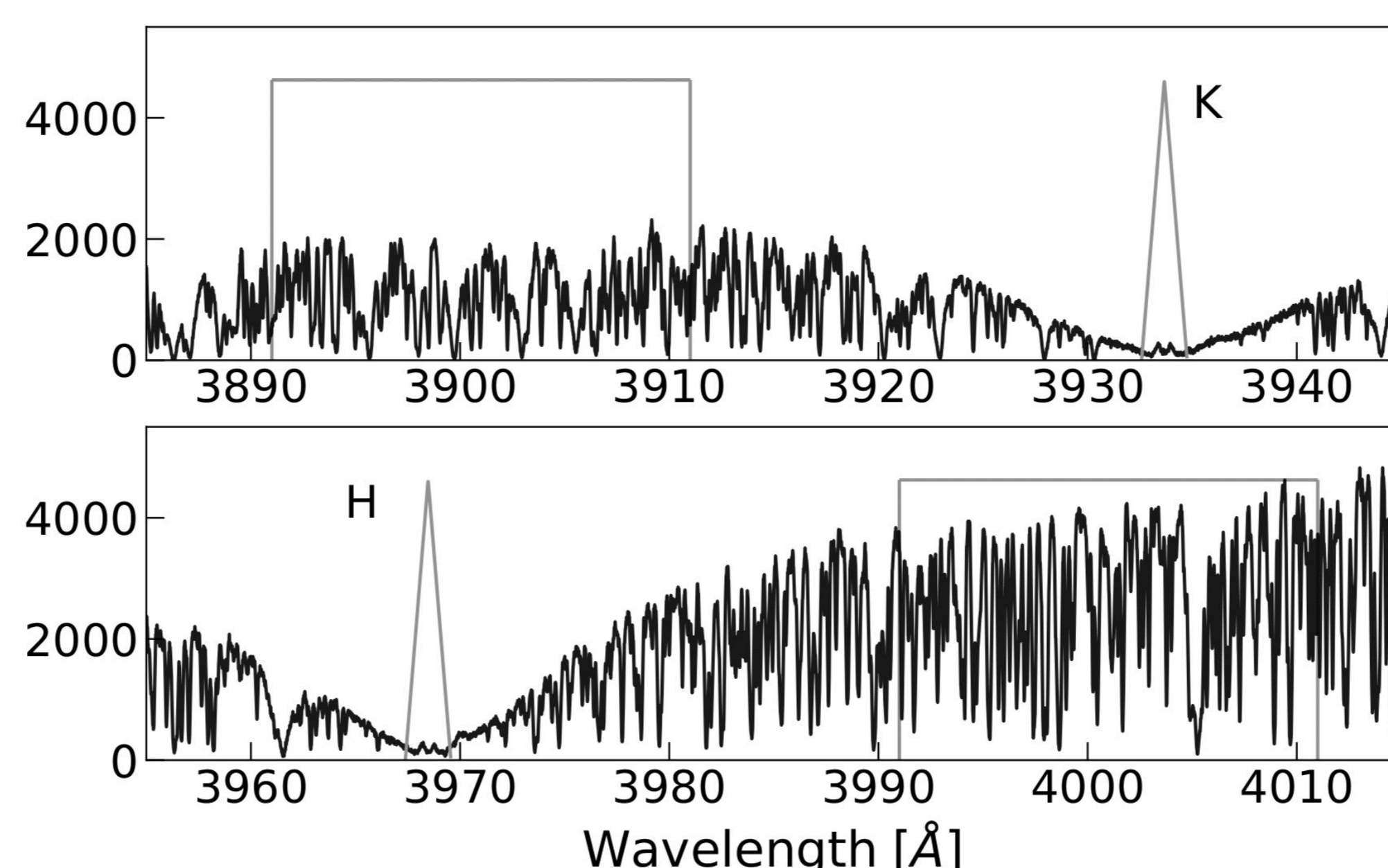


Fig 1. Example measurement of $\log R'_{HK}$ for HD 47536. We first compute the S index as sum of flux in the Call H&K lines normalized by a red and blue continuum region [2] and then converted into $\log R'_{HK}$ following [3].

We select 15 main sequence stars that are homogeneously distributed in the temperature-activity parameter space. The region $T_{\text{eff}}=4000\text{--}4500\text{ K}$ and $\log R'_{HK} < -5.0$ contains only stars that have evolved off the main sequence, hence it is not represented.

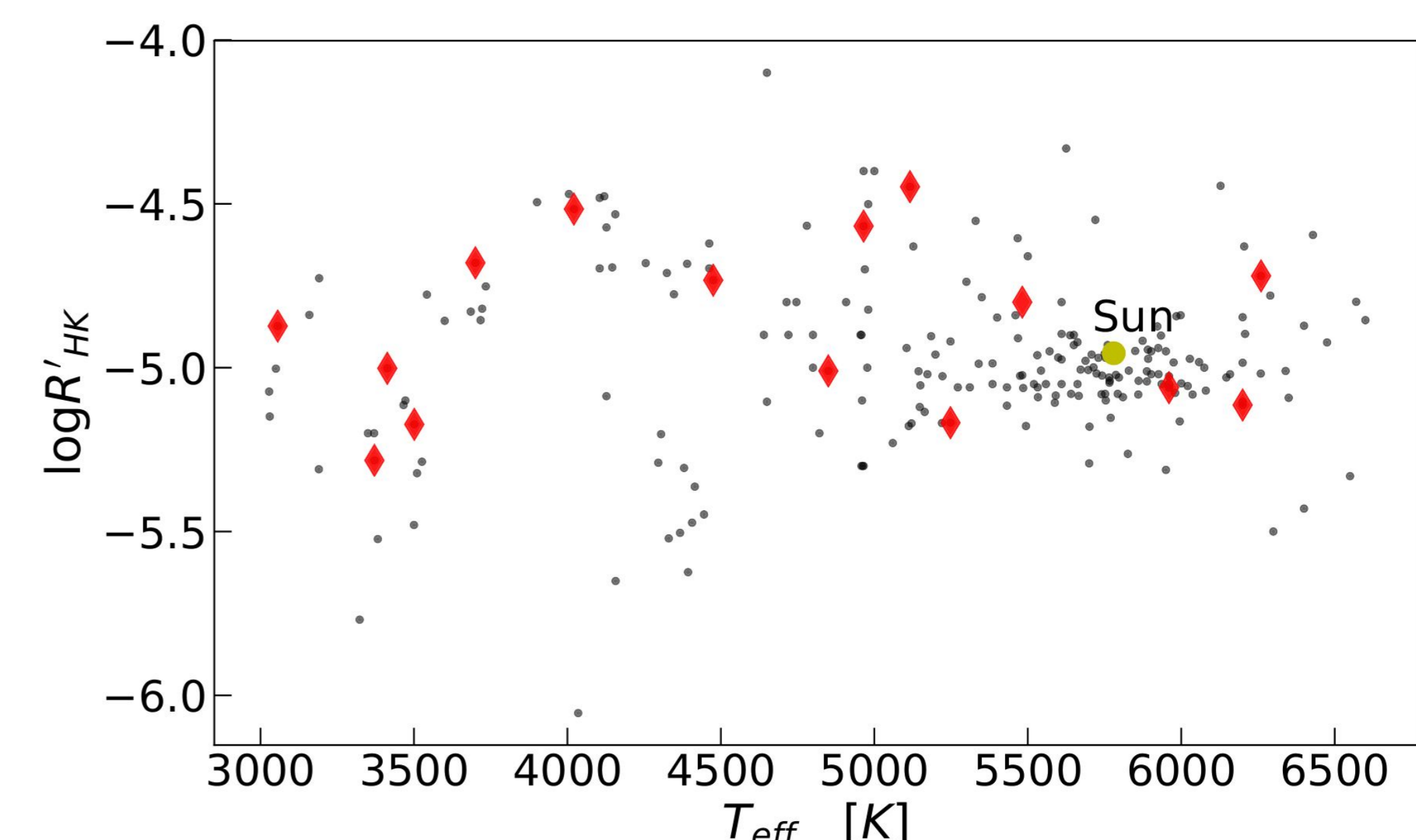


Fig. 2 Simulation sample (red diamonds) of 15 known host stars in the $\log R'_{HK}$ vs T_{eff} parameter space.

Input parameters and simulations

From empirical relations:

- Spot temperature [4,5]
- Stellar rotation period [6]

From observational estimates :

- Spot filling factor [7,8]
- Active latitudes [9]

Estimating the filling factor (f) is not straightforward, as there is no empirical relation expressing it as a function of $\log R'_{HK}$. We therefore identify three regions in the $\log R'_{HK}$ vs T_{eff} space representing observed f values over F to M spectral types above $\log R'_{HK} = -4.5$. We then 1) extrapolate these regions towards lower activity levels, taking into account that the number of spots decreases with activity, and 2) measure individual f values knowing that this quantity peaks for K stars and decreases quadratically for both hotter and cooler stars. This procedure is necessary given the paucity and often contradictory data on the filling factor for stars other than the Sun.

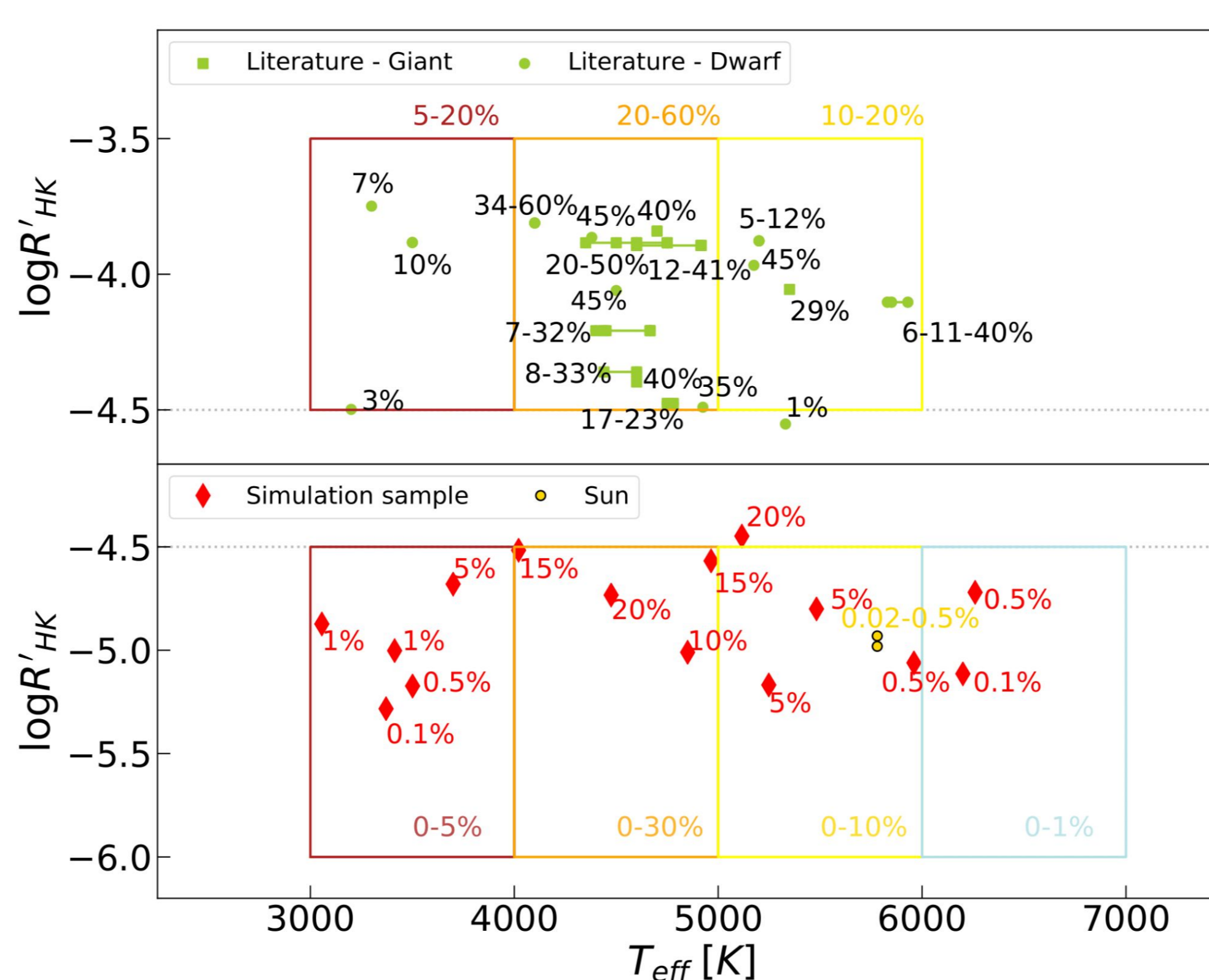


Fig. 3 Procedure adopted to estimate the spot filling factors for our simulation sample. Top: Observational data for giant (green squares) and main sequence (green circles) stars. Multiple values for an individual star are connected, and both maximum and minimum are reported. The squared boxes represent the range of typical f values over different spectral types, with associated values displayed on the top. Bottom: Extrapolation to the simulation sample. The squared boxes represent the extrapolated ranges of filling factors (given at the bottom of each box). The simulation sample is shown (red diamonds) along with the estimates of f .

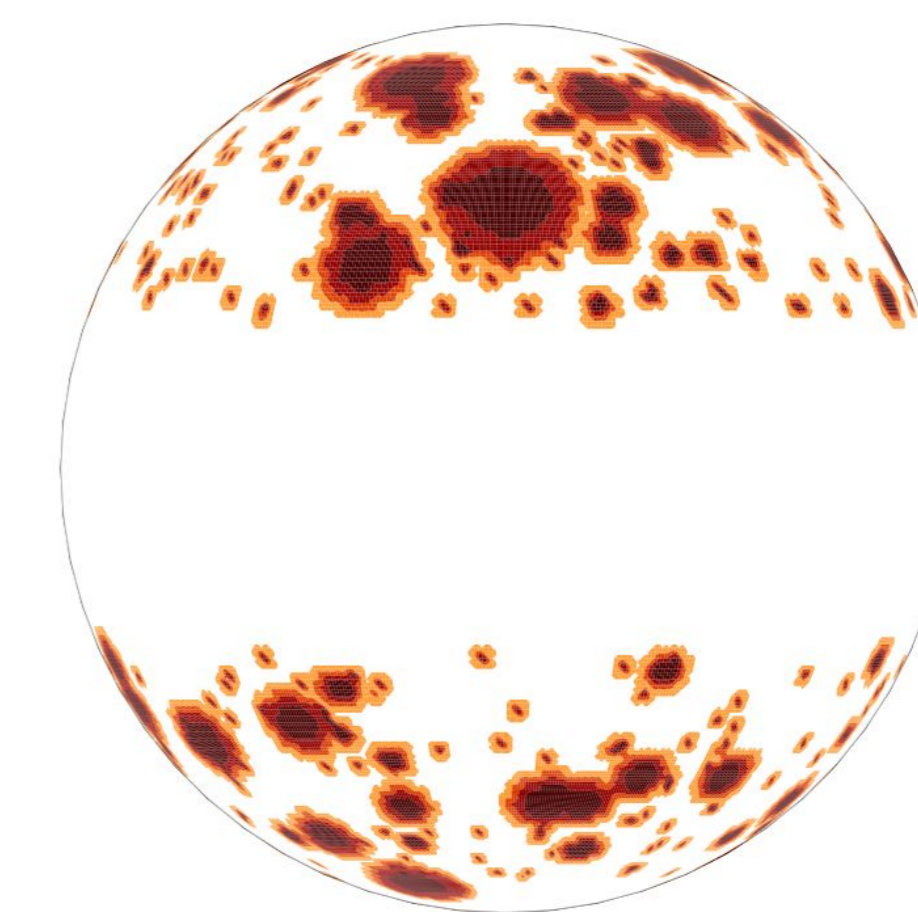


Fig. 4 Example surface map for ϵ Eridani, with a filling factor of 20%.

We simulate 150 spotted surface maps for each sample star using SPOTSS and DEEMA [10] based on the input parameters. Each map is associated with 20 synthetic spectra (one for each rotational phase).

For each surface map, we apply cross-correlation between the spectra and a template spectrum (the one at rotational phase=0.0) to obtain the spot-induced RV curve. The DEEMA code provides also V-band light curves.

Results and conclusions

From the simulated RV and light curves, we compute the mean, maximum and minimum peak-to-peak amplitude.

Our results, summarized in Fig 5., can be used as reference to determine typical peak-to-peak spot-induced RV jitter in the visible domain that can be expected when targeting host stars with different properties.

In addition, we observe:

- a positive correlation between the RV and photometric amplitude, as expected from previous studies [11].
- a reasonable agreement between our estimates and observed values (e.g. ϵ Eri, [12]), with discrepancies mainly related to the limits of our model (lack of robust filling factor information and exclusion of faculae contribution)

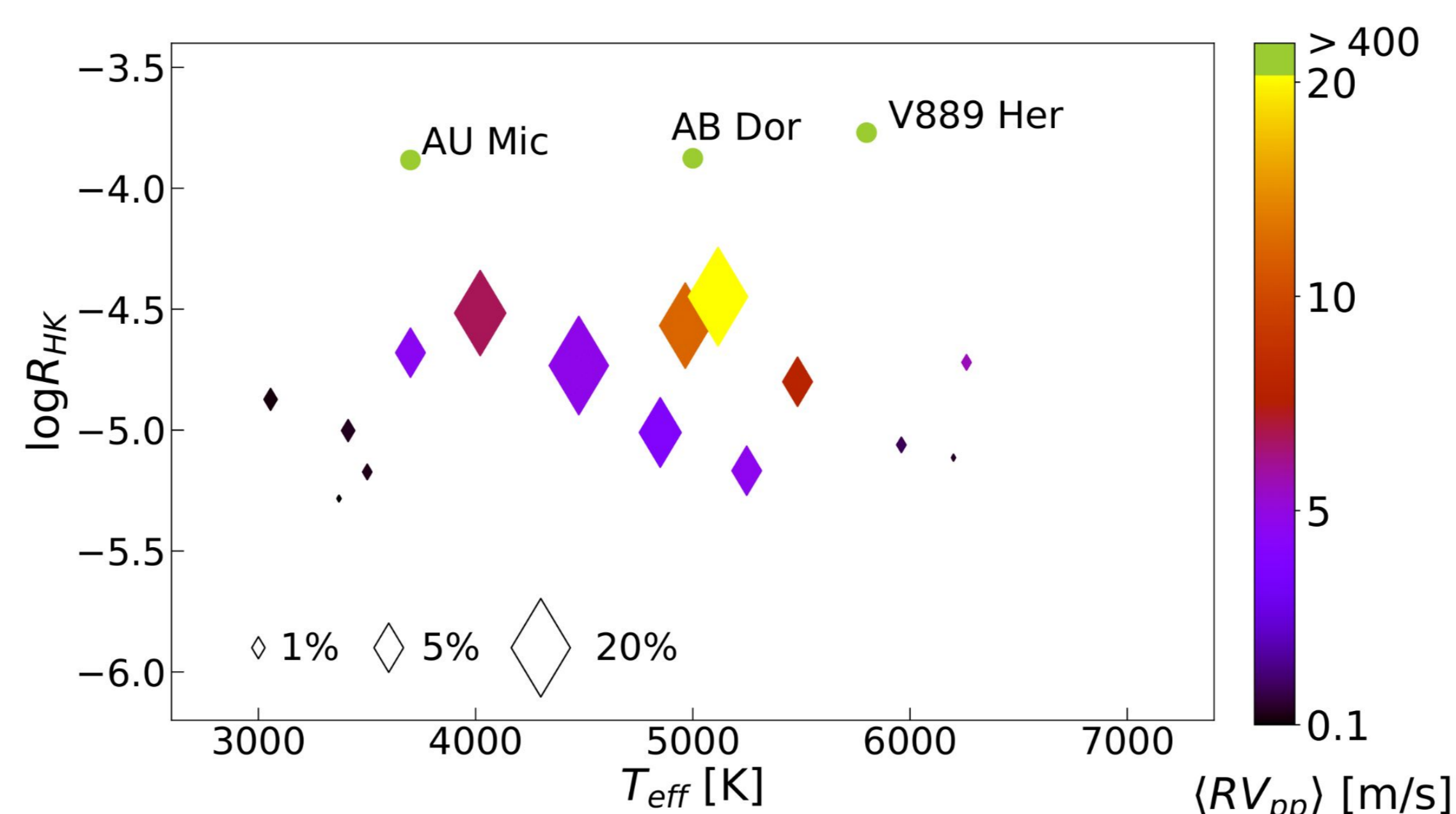


Fig. 5 The sample of 15 simulated host stars and corresponding spot-induced RV jitter. Data point size and colour encode the spot filling factor and RV jitter amplitude, respectively. Three active stars (AU Mic, AB Dor and V889 Her) are included in green for a comparison of activity level and jitter with respect to our sample (not size-scaled by the filling factor).

- the importance of target selection for small planet searches given the non-negligible RV signal even for the lowest active stars in our sample.

ID	$\langle RV_{pp} \rangle_{\text{min}}$ [m/s]	$\langle RV_{pp} \rangle_{\text{max}}$ [m/s]	$\langle RV_{pp} \rangle$ [m/s]	ΔI_{min} [mmag]	ΔI_{max} [mmag]	$\langle \Delta I \rangle$ [mmag]
YZ Cet	0.2	2.0	0.6±0.3	2.4	24.4	7.7±3.6
GJ 180	0.04	1.8	0.3±0.3	0.3	15.1	2.6±2.3
GJ 687	0.2	2.8	0.8±0.4	1.6	20.9	6.4±3.3
GJ 3634	0.3	2.7	0.7±0.3	1.1	15.6	4.5±1.8
GJ 649	2.0	17.0	6.7±2.7	5.2	51.4	21.8±9.0
HIP 54373	4.0	19.7	9.8±3.4	10.9	63.2	30.5±12.7
HIP 90979	2.9	21.2	7.0±2.6	20.0	134.2	57.1±20.3
HD 156668	2.0	18.2	6.0±2.1	15.8	100.2	43.0±14.6
HD 192263	5.4	32.9	15.9±5.5	20.6	147.2	56.7±21.5
ϵ Eri	6.3	53.6	21.6±7.5	9.0	96.0	39.9±14.7
HD 11964	0.9	16.0	6.8±2.9	3.4	80.4	35.1±15.4
HD 49674	4.0	29.7	11.5±4.5	8.5	88.0	34.8±13.6
HAT-P-5	0.4	5.1	1.5±0.8	2.1	30.6	9.7±4.7
WASP-1	0.1	9.4	0.9±1.0	0.4	41.2	4.3±4.6
HD 179949	1.8	43.2	8.2±6.5	1.6	43.0	8.6±5.9

Bibliography

- [1] Krejcová & Budaj 2012, *A&A*, 540, A82.
- [2] Vaughan 1978, *PASP*, 90, 267-274.
- [3] Middelkoop 1982, *A&A*, 107, 31-35.
- [4] Berdyugina 2005, *Living Reviews in Solar Physics*, 2, 8.
- [5] Andersen & Korhonen 2015, *MNRAS*, 448, 3053-3069.
- [6] Noyes et al. 1984, *ApJ*, 287, 769-773.
- [7] Balmaceda et al. 2009, *Journal of Geophysical Research*, 114, A07104
- [8] Afram & Berdyugina 2015, *A&A*, 576, A34.
- [9] Granzer et al. 2000, *A&A*, 355, 1087-1097.
- [10] Korhonen et al. 2015, *MNRAS*, 448, 3038-3052.
- [11] Hojjatpanah et al. 2020, *A&A*, 639, A35.
- [12] Petit et al. 2021, *A&A*, 648, A55.